International Journal of Geometric Methods in Modern Physics
Vol. 20, No. 2 (2023) 2350035 (22 pages)

DOI: 10.1142/S0219887823500354

On Hosoya polynomial and subsequent indices of pent–heptagonal carbon nanosheets

Umber Sheikh

Department of Mathematics
Division of Science and Technology
University of Education, Lahore, Pakistan
umber.sheikh@ue.edu.pk

Sidra Rashid

Department of Applied Sciences
National Textile University
Faisalabad, Pakistan
2019ntumsmm3024@ntu.edu.pk

Cenap Ozel

Department of Mathematics
King Abdulaziz University
Jeddah, Makkah, Kingdom of Saudi Arabia
cozel@kau.edu.sa

Richard Pincak*

Institute of Experimental Physics
Slovak Academy of Sciences, Košice, Slovakia
pincak@saske.sk

Received 31 August 2022
Accepted 22 September 2022
Published 7 November 2022

The pent–heptagonal carbon nanosheets (CNSs) admit significant industrial applications. We shall compute the distance-based Hosoya polynomial of CNSs including VC_5C_7 and HC_5C_7. The first-, second- and third-order derivatives of Hosoya polynomial, respectively, lead to the Wiener, hyper-Wiener and Tratch–Stankevitch–Zefirov (TSZ) indices which are the distance-based topological indices. These indices have many physical applications and can be correlated to physio-chemical properties of chemical structures. Results exhibit that despite the fact that both sheets have the same chemical formula, they have different Hosoya polynomials and related distance-based topological indices,

*Corresponding author.

resulting in distinct quantitative structure–property relation (QSPR) and quantitative structure–activity relation (QSAR) due to configuration differences.

Keywords: Pent–heptagonal carbon nanosheets; Hosoya polynomial; Wiener index; hyper-Wiener index; Tratch–Stankevitch–Zefirov index.

Mathematics Subject Classification 2020: 05C12, 05C31, 05C90, 92E10

1. Introduction

Nanostructures are structures of tiny dimensions in the nanometer range (1–100 nm), admitting distinct and intriguing properties that distinguish them from their bulk counterparts. The nanostructures are categorized by their size, shape and topology. Carbon-based nanostructures (CBNs) are significant due to their unique features like thermal and electrical conductivity, high mechanical strength, optical qualities [1, 2]. CBNs include carbon nanosheets (CNSs), graphene, fullerenes, nanospheres, nanobuds, nanotubes, nanowires, nanoribbons, nanofoam, nanocone, nanochain and nanotorus. CBNs are developed for industrial and biological engineering applications due to their favorable features [3–5].

CNSs are important due to their flexible and stable uniformly thick structures. CNSs admit applications in sensors, filtration membranes, sample supports and conductive coatings [6]. Moreover, they have possible applications including batteries, transistors, water filtration, antennas, supercapacitors, touch-screens, solar cells, electrocatalytic oxygen reductions and DNA sequencing [7–9]. A novelty in the field are the porous CNSs admitting high surface area, controlled doping and good electrical conductivity. They are used in lithium ion batteries, electrocatalytic oxygen reductions, supercapacitors and in many energy-related applications [10–12].

Topological indices are the molecular descriptors indicating numerical values with clear structural interpretation to describe the complex molecular properties. A correlation between an index and a single molecular property may reveal the structural makeup of that feature. In mathematical chemistry, molecular descriptors serve an important role in quantitative structure–property relations (QSPRs) and quantitative structure–activity relations (QSARs) studies. The first introduced distance-based topological index was the Wiener index and is defined as [13]

$$W(G) = \Sigma_{(u,v)\in V(G)}\triangle, \tag{1}$$

where u and v are the vertices of graph G and $\triangle$ is the distance (minimum number of edges traversed) between the two vertices. Wiener index helps in determining the boiling points of alkanes. Moreover, QSAR implies that this index correlates the physical properties of alkane to its critical point, density, surface tension and viscosity [14].

The creation of several more topological indices was sparked by the Wiener index. A development of the Wiener index is the hyper-Wiener index and defined mathematically as [15]

$$\mathrm{HW}(G) = \Sigma_{(u,v)\in V(G)} \triangle(1+\triangle). \tag{2}$$

The hyper-Wiener index reduces a particle's structure to a number that indicates subatomic stretching and electronic structures. The Tratch–Stankevitch–Zefirov (TSZ) index can be written as [16]

$$\mathrm{TSZ}(G) = \Sigma \frac{1}{6}(2\triangle + 3\triangle^2 + \triangle^3). \tag{3}$$

The TSZ index is the extended Wiener index [17].

A popular distance-based algebraic polynomial is the Hosoya polynomial [18]. Many chemical applications exist for the Hosoya polynomial [19]. The Hosoya polynomial in variable y for a simply connected graph G is defined as

$$H(G,y) = \Sigma_{(u,v)\in V(G)} y^{\triangle}. \tag{4}$$

A majority of distance-based topological indices are computed from this polynomial [13, 20]. Since Wiener, hyper-Wiener and TSZ indices are distance-based, therefore all of these can be derived from the closed form known as Hosoya polynomial.

Molecular graphs are used to mathematically simulate chemical structures. The topological structure of molecules, represented mathematically as molecular graphs, is connected to the graph invariants including algebraic polynomials and topological indices [21]. A graph invariant numerically characterizes a molecule's topological structure. The Hosoya index is a polynomial graph invariant and is determined by counting non-incident edges in a graph.

Hosoya polynomial and computation of corresponding topological indices has been recently in fashion. A recent novelty is to solve Volterra–Fredholm integral equations with Hosoya polynomials [22]. Hosoya polynomials of TOX, RTOX, TSL and RTSL have been investigated [23]. Hosoya polynomials has been investigated for n-bilinear straight pentachain structures [24], capped armchair nanotubes [25], TUC_4 nanotube [26], $C_4C_8(R)$ and $C_4C_8(S)$ nanosheets [27] and single walled (n,m) carbon nanotubes [28]. The corresponding topological indices including Weiner and hyper-Weiner indices of nanostructures have also been of interest [29, 30].

In the recent era the topological indices are used to predict the physico-chemical properties of the COVID-19 vaccine [31–35]. It is worth noting that no-one has investigated the Hosoya polynomial and related distance-based topological indices of pent–heptagonal CNSs $VC_5C_7[p,q]$, $HC_5C_7[p,q]$.

In this work, the Hosoya polynomial of penta–heptagonal CNS structures, comprising VC_5C_7 and HC_5C_7, is computed. The molecular graphs are formed which reveal the lattice of a molecule. The Hosoya polynomial displays the molecular graph's symmetries and thus, the crystal symmetries. The MAPLE software is used to determine the first-, second- and third-order derivatives of the Hosoya polynomial leading to the Wiener, hyper-Wiener and TSZ indices, respectively. Additionally given is the visual examination of the topological indices for the two CNS.

2. Methodology

Take into account a molecular graph $G = G(V(G)), (E(G))$ with finite nonempty sets of vertices $(V(G))$ and edges $(E(G))$. The topology of the chemical structure of a molecule is displayed in the molecular graph. Let $\triangle$ presents the distance between any pair of vertices of graph G. For the sake of Hosoya polynomial and corresponding indices, we shall proceed in the following manner:

- We shall compute the frequency of pair of vertices at distance $1, 2, 3, 4, \ldots, d(G)$, where $d(G) = \max \triangle$; for all $u, v \in V(G)$.
- The general expression for a Hosoya polynomial is

$$H(G, y) = |l_1(\mathfrak{q})|y + |l_2(\mathfrak{q})|y^2 + \cdots + |l_d(\mathfrak{q})|y^d = \Sigma_{k=1}^{d} |l_k(\mathfrak{q})|y^k, \tag{5}$$

  where $|l_k(n)|$ is the number of pair of vertices at distance k and d is the maximum of the distances between the pair of vertices. The vertices' separations from one another will be organized in matrix form. It will be possible to deduce the matrix's general form. In order to determine the coefficient of the kth term of the Hosoya polynomial, the number of vertices with the same distance $|l_k(\mathfrak{q})|$ will be determined.
- Using differential calculus, this polynomial will be utilized to calculate the topological indices, including the Wiener, hyper-Wiener and TSZ indices.
  - — The Wiener index can be calculated as the first derivative of Hosoya polynomial taking the value of variable as unity and can be expressed as [36]

$$W(G) = \frac{d}{dy} H(G, y)|_{y=1}. \tag{6}$$

  - — The hyper-Wiener index can also be deduced from the Hosoya polynomial via the following formula [36]:

$$\mathrm{HW}(G) = \frac{1}{2} \frac{d^2}{dy^2} H(G, y)|_{y=1}. \tag{7}$$

  - — The TSZ index can be calculated as the third derivative of Hosoya polynomial under the following relationship [37]:

$$\mathrm{TSZ}(G) = \frac{1}{6} \frac{d^3}{dy^3} H(G, y)|_{y=1}. \tag{8}$$

  It is worthy to mention that in all the three equations (6)–(8), the limit $y = 1$ leads to the sum of coefficients substituting $y = 1$.

3. Computational Results

This section is devoted to the calculation of Hosoya polynomial and related indices of the pent–heptagonal CNS including VC_5C_7 and HC_5C_7. The structure of C_5C_7 is a two-dimensional lattice consisting of numerous compounds by alternating C_5

and C_7. The structure C_5 represents a pentagon and C_7 represents a heptagon in the graph. The computations of Hosoya polynomial and related topological indices for the two CNS, VC_5C_7 and HC_5C_7 are presented in the form of theorems and corollaries.

3.1. *Pent–heptagonal CNS VC_5C_7*

A VC_5C_7 is the vertical arrangement of CNS C_5C_7. Thus, a two-dimensional lattice is developed which entertains C_5 as pentagon and C_7 as heptagon in VC_5C_7 as shown in Fig. 1. It is noteworthy that in the arrangement $VC_5C_7[\mathfrak{q}],\ \mathfrak{q} > 1,\ \mathfrak{q}\epsilon\mathbb{N}$ is the length of the sheet.

Theorem 1. *For the topology of pent–heptagonal CNS VC_4C_8, the Hosoya polynomial is calculated as*

$$\begin{aligned} H(VC_5C_7, y) = {} & (72\mathfrak{q}+2)y + (120\mathfrak{q}-2)y^2 + (152\mathfrak{q}-6)y^3 \\ & + (148\mathfrak{q}-14)y^4 + \Sigma_{w=1}^{\mathfrak{q}} 32((4\mathfrak{q}-w)+10)y^{6w-1} \\ & + \Sigma_{w=1}^{\mathfrak{q}} 33((4\mathfrak{q}-w)+6)y^{6w} + \Sigma_{w=1}^{\mathfrak{q}} 34((4\mathfrak{q}-w)+2)y^{6w+1} \\ & + \Sigma_{w=1}^{\mathfrak{q}} 33((4\mathfrak{q}-w)-2)y^{6w+2} + \Sigma_{w=1}^{\mathfrak{q}} 32((4\mathfrak{q}-w)-6)y^{6w+3} \\ & + \Sigma_{w=1}^{\mathfrak{q}} 32((4\mathfrak{q}-w)-14)y^{6w+4}. \end{aligned} \tag{9}$$

Proof. The distance matrix D corresponding to the molecular graph of CNS VC_5C_7 is

$$D = \begin{bmatrix} B_0 & B_1 & B_2 & B_3 & B_4 & B_5 & \dots & B_{3\mathfrak{q}-1} & C_{3\mathfrak{q}} \\ B_1^T & A_0 & A_1 & A_2 & A_3 & A_4 & \dots & A_{3\mathfrak{q}-2} & C_{3\mathfrak{q}-1} \\ B_2^T & A_1^T & A_0 & A_1 & A_2 & A_3 & \dots & A_{3\mathfrak{q}-3} & C_{3\mathfrak{q}-2} \\ B_3^T & A_2^T & A_1^T & A_0 & A_1 & A_2 & \dots & A_{3\mathfrak{q}-4} & C_{3\mathfrak{q}-3} \\ B_4^T & A_3^T & A_2^T & A_1^T & A_0 & A_1 & \dots & A_{3\mathfrak{q}-5} & C_{3\mathfrak{q}-4} \\ B_5^T & A_4^T & A_3^T & A_2^T & A_1^T & A_o & \dots & A_{3\mathfrak{q}-6} & C_{3\mathfrak{q}-5} \\ . & . & . & . & . & . & . & . & \\ . & . & . & . & . & . & . & . & \\ . & . & . & . & . & . & . & . & \\ B_{3\mathfrak{q}-1}^T & A_{3\mathfrak{q}-2}^T & A_{3\mathfrak{q}-3}^T & A_{3\mathfrak{q}-4}^T & A_{3\mathfrak{q}-5}^T & A_{3\mathfrak{q}-6}^T & \dots & A_0 & C_1 \\ C_{3\mathfrak{q}}^T & C_{3\mathfrak{q}-1}^T & C_{3\mathfrak{q}-2}^T & C_{3\mathfrak{q}-3}^T & C_{3\mathfrak{q}-4}^T & C_{3\mathfrak{q}-5}^T & \dots & C_1^T & C_0 \end{bmatrix}_{1\le w\le 3\mathfrak{q}},$$

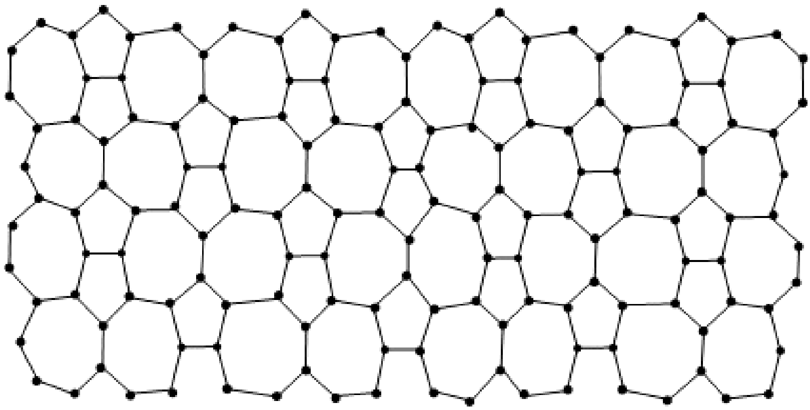

Fig. 1. The molecular graph of CNS VC_5C_7.

where $A_0, A_1, A_2, A_3, A_4, A_5, \ldots, A_{3\mathfrak{q}-2}$, $B_0, B_1, B_2, B_3, B_4, B_5, \ldots, B_{3\mathfrak{q}-1}$ and $C_0, C_1, C_2, C_3, C_4, C_5, \ldots, C_{3\mathfrak{q}}$ are the submatrices. These matrices can be computed as follows ($\clubsuit = 6\mathfrak{q}$):

$$A_0 = \begin{bmatrix} 0 & 1 & 1 & 2 & 3 & 3 & 2 & 3 & 4 & 4 & 5 & 4 & 5 & 6 \\ 1 & 0 & 2 & 3 & 3 & 2 & 1 & 4 & 5 & 4 & 4 & 3 & 6 & 5 \\ 1 & 2 & 0 & 1 & 2 & 3 & 3 & 2 & 3 & 4 & 4 & 4 & 4 & 5 \\ 2 & 3 & 1 & 0 & 1 & 2 & 3 & 1 & 2 & 2 & 3 & 3 & 3 & 4 \\ 3 & 3 & 2 & 1 & 0 & 1 & 2 & 2 & 2 & 1 & 2 & 2 & 3 & 3 \\ 3 & 2 & 3 & 2 & 1 & 0 & 1 & 3 & 3 & 2 & 2 & 1 & 4 & 3 \\ 2 & 1 & 3 & 3 & 2 & 1 & 0 & 4 & 4 & 3 & 3 & 2 & 5 & 4 \\ 3 & 4 & 2 & 1 & 2 & 3 & 4 & 0 & 1 & 2 & 3 & 4 & 2 & 4 \\ 4 & 5 & 3 & 2 & 2 & 3 & 4 & 1 & 0 & 1 & 2 & 3 & 1 & 3 \\ 4 & 4 & 3 & 2 & 1 & 2 & 3 & 2 & 1 & 0 & 1 & 2 & 2 & 2 \\ 5 & 4 & 4 & 3 & 2 & 2 & 3 & 3 & 2 & 1 & 0 & 1 & 3 & 1 \\ 4 & 3 & 4 & 3 & 2 & 1 & 2 & 4 & 3 & 2 & 1 & 0 & 4 & 2 \\ 5 & 6 & 4 & 3 & 3 & 4 & 5 & 2 & 1 & 2 & 3 & 4 & 0 & 3 \\ 6 & 5 & 5 & 4 & 3 & 3 & 4 & 4 & 3 & 2 & 1 & 2 & 3 & 0 \end{bmatrix},$$

$$A_k = \left[\begin{array}{cccccccccccccc}
\clubsuit & \clubsuit+1 & \clubsuit+1 & \clubsuit+2 & \clubsuit+3 & \clubsuit+3 & \clubsuit+2 & \clubsuit+3 & \clubsuit+4 & \clubsuit+4 & \clubsuit+5 & \clubsuit+4 & \clubsuit+5 & \clubsuit+6 \\
\clubsuit+1 & \clubsuit & \clubsuit+2 & \clubsuit+3 & \clubsuit+3 & \clubsuit+2 & \clubsuit+1 & \clubsuit+4 & \clubsuit+5 & \clubsuit+4 & \clubsuit+4 & \clubsuit+3 & \clubsuit+6 & \clubsuit+5 \\
\clubsuit-1 & \clubsuit & \clubsuit & \clubsuit+1 & \clubsuit+2 & \clubsuit+2 & \clubsuit+1 & \clubsuit+2 & \clubsuit+3 & \clubsuit+3 & \clubsuit+4 & \clubsuit+3 & \clubsuit+4 & \clubsuit+5 \\
\clubsuit-2 & \clubsuit-1 & \clubsuit-1 & \clubsuit & \clubsuit+1 & \clubsuit+1 & \clubsuit & \clubsuit+1 & \clubsuit+2 & \clubsuit+2 & \clubsuit+3 & \clubsuit+2 & \clubsuit+3 & \clubsuit+4 \\
\clubsuit-2 & \clubsuit-2 & \clubsuit-1 & \clubsuit & \clubsuit+1 & \clubsuit & \clubsuit-1 & \clubsuit+1 & \clubsuit+2 & \clubsuit+2 & \clubsuit+2 & \clubsuit+1 & \clubsuit+3 & \clubsuit+3 \\
\clubsuit-1 & \clubsuit-2 & \clubsuit & \clubsuit+1 & \clubsuit+1 & \clubsuit & \clubsuit-1 & \clubsuit+2 & \clubsuit+3 & \clubsuit+2 & \clubsuit+2 & \clubsuit+1 & \clubsuit+4 & \clubsuit+3 \\
\clubsuit & \clubsuit-1 & \clubsuit+1 & \clubsuit+2 & \clubsuit+2 & \clubsuit+1 & \clubsuit & \clubsuit+3 & \clubsuit+4 & \clubsuit+3 & \clubsuit+3 & \clubsuit+2 & \clubsuit+5 & \clubsuit+4 \\
\clubsuit-3 & \clubsuit-2 & \clubsuit-2 & \clubsuit-1 & \clubsuit & \clubsuit & \clubsuit-1 & \clubsuit & \clubsuit+1 & \clubsuit+1 & \clubsuit+2 & \clubsuit+1 & \clubsuit+2 & \clubsuit+3 \\
\clubsuit-4 & \clubsuit-3 & \clubsuit-3 & \clubsuit-2 & \clubsuit-1 & \clubsuit-1 & \clubsuit-2 & \clubsuit-1 & \clubsuit & \clubsuit & \clubsuit+1 & \clubsuit & \clubsuit+1 & \clubsuit+2 \\
\clubsuit-3 & \clubsuit-3 & \clubsuit-2 & \clubsuit-1 & \clubsuit & \clubsuit-1 & \clubsuit-2 & \clubsuit & \clubsuit+1 & \clubsuit+1 & \clubsuit+1 & \clubsuit & \clubsuit+2 & \clubsuit+2 \\
\clubsuit-3 & \clubsuit-4 & \clubsuit-2 & \clubsuit-1 & \clubsuit-1 & \clubsuit-2 & \clubsuit-3 & \clubsuit & \clubsuit+1 & \clubsuit & \clubsuit & \clubsuit-1 & \clubsuit+2 & \clubsuit+1 \\
\clubsuit-2 & \clubsuit-3 & \clubsuit-1 & \clubsuit & \clubsuit & \clubsuit-1 & \clubsuit-2 & \clubsuit+1 & \clubsuit+2 & \clubsuit+1 & \clubsuit+1 & \clubsuit & \clubsuit+3 & \clubsuit+2 \\
\clubsuit-5 & \clubsuit-4 & \clubsuit-4 & \clubsuit-3 & \clubsuit-2 & \clubsuit-2 & \clubsuit-3 & \clubsuit-2 & \clubsuit-1 & \clubsuit-1 & \clubsuit & \clubsuit-1 & \clubsuit & \clubsuit+1 \\
\clubsuit-4 & \clubsuit-5 & \clubsuit-3 & \clubsuit-2 & \clubsuit-2 & \clubsuit-3 & \clubsuit-4 & \clubsuit-1 & \clubsuit & \clubsuit-1 & \clubsuit-1 & \clubsuit-2 & \clubsuit+1 & \clubsuit
\end{array}\right]_{1 \le k \le \frac{\clubsuit}{2}-2},$$

$$B_0 = \begin{bmatrix} 0 & 1 & 2 & 3 & 3 & 2 & 1 & 3 & 4 & 4 & 5 & 4 & 5 & 6 \\ 1 & 0 & 1 & 2 & 3 & 3 & 2 & 2 & 3 & 3 & 4 & 4 & 4 & 5 \\ 2 & 1 & 0 & 1 & 2 & 3 & 3 & 1 & 2 & 2 & 3 & 3 & 3 & 4 \\ 3 & 2 & 1 & 0 & 1 & 2 & 3 & 2 & 2 & 1 & 2 & 2 & 3 & 3 \\ 3 & 3 & 2 & 1 & 0 & 1 & 2 & 3 & 3 & 2 & 2 & 1 & 4 & 3 \\ 2 & 3 & 3 & 2 & 1 & 0 & 1 & 4 & 4 & 3 & 3 & 2 & 5 & 4 \\ 1 & 2 & 3 & 3 & 2 & 1 & 0 & 4 & 5 & 4 & 4 & 3 & 6 & 5 \\ 3 & 2 & 1 & 2 & 3 & 4 & 4 & 0 & 1 & 2 & 3 & 4 & 2 & 4 \\ 3 & 3 & 2 & 2 & 3 & 4 & 4 & 1 & 0 & 1 & 2 & 3 & 1 & 3 \\ 4 & 3 & 2 & 1 & 2 & 3 & 4 & 2 & 1 & 0 & 1 & 2 & 2 & 2 \\ 5 & 4 & 3 & 2 & 2 & 3 & 4 & 3 & 2 & 1 & 0 & 1 & 3 & 1 \\ 4 & 4 & 3 & 2 & 1 & 2 & 3 & 4 & 3 & 2 & 1 & 0 & 4 & 2 \\ 5 & 4 & 3 & 3 & 4 & 5 & 6 & 2 & 1 & 2 & 3 & 4 & 0 & 3 \\ 6 & 5 & 4 & 3 & 3 & 4 & 5 & 4 & 3 & 2 & 1 & 2 & 3 & 0 \end{bmatrix},$$

$$B_k = \left[\begin{array}{cccccccc} \clubsuit & \clubsuit+1 & \clubsuit+1 & \clubsuit+2 & \clubsuit+3 & \clubsuit+3 & \clubsuit+2 & \clubsuit+3 \\ \clubsuit-1 & \clubsuit & \clubsuit & \clubsuit+1 & \clubsuit+2 & \clubsuit+2 & \clubsuit+1 & \clubsuit+2 \\ \clubsuit-2 & \clubsuit-1 & \clubsuit-1 & \clubsuit & \clubsuit+1 & \clubsuit+1 & \clubsuit & \clubsuit+1 \\ \clubsuit-2 & \clubsuit-2 & \clubsuit-1 & \clubsuit & \clubsuit+1 & \clubsuit & \clubsuit-1 & \clubsuit+1 \\ \clubsuit-1 & \clubsuit-2 & \clubsuit & \clubsuit+1 & \clubsuit+1 & \clubsuit & \clubsuit-1 & \clubsuit+2 \\ \clubsuit & \clubsuit-1 & \clubsuit+1 & \clubsuit+2 & \clubsuit+2 & \clubsuit+1 & \clubsuit & \clubsuit+3 \\ \clubsuit+1 & \clubsuit & \clubsuit+2 & \clubsuit+3 & \clubsuit+3 & \clubsuit+2 & \clubsuit+1 & \clubsuit+4 \\ \clubsuit-3 & \clubsuit-2 & \clubsuit-2 & \clubsuit-1 & \clubsuit & \clubsuit & \clubsuit-1 & \clubsuit \\ \clubsuit-4 & \clubsuit-3 & \clubsuit-3 & \clubsuit-2 & \clubsuit-1 & \clubsuit-1 & \clubsuit-2 & \clubsuit-1 \\ \clubsuit-3 & \clubsuit-3 & \clubsuit-2 & \clubsuit-1 & \clubsuit & \clubsuit-1 & \clubsuit-2 & \clubsuit \\ \clubsuit-3 & \clubsuit-4 & \clubsuit-2 & \clubsuit-1 & \clubsuit-1 & \clubsuit-2 & \clubsuit-3 & \clubsuit \\ \clubsuit-2 & \clubsuit-3 & \clubsuit-1 & \clubsuit & \clubsuit & \clubsuit-1 & \clubsuit-2 & \clubsuit+1 \\ \clubsuit-5 & \clubsuit-4 & \clubsuit-4 & \clubsuit-3 & \clubsuit-2 & \clubsuit-2 & \clubsuit-3 & \clubsuit-2 \\ \clubsuit-4 & \clubsuit-5 & \clubsuit-3 & \clubsuit-2 & \clubsuit-2 & \clubsuit-3 & \clubsuit-4 & \clubsuit-1 \end{array}\right.$$

$$\left.\begin{matrix}
\clubsuit+4 & \clubsuit+4 & \clubsuit+5 & \clubsuit+4 & \clubsuit+5 & \clubsuit+6\\
\clubsuit+3 & \clubsuit+3 & \clubsuit+4 & \clubsuit+3 & \clubsuit+4 & \clubsuit+5\\
\clubsuit+2 & \clubsuit+2 & \clubsuit+3 & \clubsuit+2 & \clubsuit+3 & \clubsuit+4\\
\clubsuit+2 & \clubsuit+2 & \clubsuit+2 & \clubsuit+1 & \clubsuit+3 & \clubsuit+3\\
\clubsuit+3 & \clubsuit+2 & \clubsuit+2 & \clubsuit+1 & \clubsuit+4 & \clubsuit+3\\
\clubsuit+4 & \clubsuit+3 & \clubsuit+3 & \clubsuit+2 & \clubsuit+5 & \clubsuit+4\\
\clubsuit+5 & \clubsuit+4 & \clubsuit+4 & \clubsuit+3 & \clubsuit+6 & \clubsuit+5\\
\clubsuit+1 & \clubsuit+1 & \clubsuit+2 & \clubsuit+1 & \clubsuit+2 & \clubsuit+3\\
\clubsuit & \clubsuit & \clubsuit+1 & \clubsuit & \clubsuit+1 & \clubsuit+2\\
\clubsuit+1 & \clubsuit+1 & \clubsuit+1 & \clubsuit & \clubsuit+2 & \clubsuit+2\\
\clubsuit+1 & \clubsuit & \clubsuit & \clubsuit-3 & \clubsuit+2 & \clubsuit+1\\
\clubsuit+2 & \clubsuit+1 & \clubsuit+1 & \clubsuit & \clubsuit+3 & \clubsuit+2\\
\clubsuit+1 & \clubsuit-1 & \clubsuit & \clubsuit-1 & \clubsuit & \clubsuit+1\\
\clubsuit & \clubsuit-1 & \clubsuit-1 & \clubsuit-2 & \clubsuit+1 & \clubsuit
\end{matrix}\right]_{1\leq k\leq \frac{\clubsuit}{2}-1},$$

$$C_0=\begin{bmatrix}0 & 1\\ 1 & 0\end{bmatrix},\quad C_k=\begin{bmatrix}
\clubsuit & \clubsuit+1\\
\clubsuit+1 & \clubsuit\\
\clubsuit-1 & \clubsuit\\
\clubsuit-2 & \clubsuit-1\\
\clubsuit-2 & \clubsuit-2\\
\clubsuit-1 & \clubsuit-2\\
\clubsuit & \clubsuit-1\\
\clubsuit-3 & \clubsuit-2\\
\clubsuit-4 & \clubsuit-3\\
\clubsuit-3 & \clubsuit-3\\
\clubsuit-3 & \clubsuit-4\\
\clubsuit-2 & \clubsuit-3\\
\clubsuit-5 & \clubsuit-4\\
\clubsuit-4 & \clubsuit-5
\end{bmatrix}_{1\leq k\leq \frac{\clubsuit}{2}}.$$

For the sake of computing $|l_k(\mathfrak{q})|$ (k is the distance between the pairs), we can calculate as follows:

$$\begin{aligned} l_1(\mathfrak{q}) &= [\#1 \in B_0] \times [\#B_0] + [\#1 \in B_1] \times [\#B_1] + [\#1 \in A_0] \times [\#A_0] \\ &\quad + [\#1 \in A_1] \times [\#A_1] + [\#1 \in C_0] \times [\#C_0] + [\#1 \in C_1] \times [\#C_1] \\ &= 16(1) + 2(1) + 16(4\mathfrak{q} - 1) + 2(4\mathfrak{q} - 2) + 2(1) + 2(1) \\ &= 16 + 2 + 64\mathfrak{q} - 16 + 8\mathfrak{q} - 4 + 4 \\ &= 72\mathfrak{q} + 2. \end{aligned}$$

Similarly,

$$\begin{aligned} &|l_2(\mathfrak{q})| = 120\mathfrak{q} - 2, && |l_3(\mathfrak{q})| = 152\mathfrak{q} - 6, \\ &|l_4(\mathfrak{q})| = 148\mathfrak{q} - 14, && |l_{6w-1}(\mathfrak{q})| = \Sigma_{w=1}^{\mathfrak{q}} 32(4n - w) + 10, \\ &|l_{6w}(\mathfrak{q})| = \Sigma_{w=1}^{\mathfrak{q}} 33(4\mathfrak{q} - w) + 6, && |l_{6w+1}(\mathfrak{q})| = \Sigma_{w=1}^{\mathfrak{q}} 34(4\mathfrak{q} - w) + 2, \\ &|l_{6w+2}(\mathfrak{q})| = \Sigma_{w=1}^{\mathfrak{q}} 33(4\mathfrak{q} - w) - 2, && |l_{6w+3}(\mathfrak{q})| = \Sigma_{w=1}^{\mathfrak{q}} 32(4\mathfrak{q} - w) - 6, \\ &|l_{6w+4}(\mathfrak{q})| = \Sigma_{w=1}^{\mathfrak{q}} 32(4\mathfrak{q} - w) - 14. \end{aligned}$$

Substituting these values into Eq. (5) leads to the following form of Hosoya polynomial for pent–heptagonal CNS VC_5C_7 as

$$\begin{aligned} H(VC_5C_7, y) &= (72\mathfrak{q} + 2)y + (120\mathfrak{q} - 2)y^2 + (152\mathfrak{q} - 6)y^3 + (148\mathfrak{q} - 14)y^4 \\ &\quad + \Sigma_{i=1}^{\mathfrak{q}} 32((4\mathfrak{q} - w) + 10)y^{6w-1} + \Sigma_{w=1}^{\mathfrak{q}} 33((4\mathfrak{q} - w) + 6)y^{6w} \\ &\quad + \Sigma_{w=1}^{\mathfrak{q}} 34((4\mathfrak{q} - w) + 2)y^{6w+1} + \Sigma_{w=1}^{\mathfrak{q}} 33((4\mathfrak{q} - w) - 2)y^{6w+2} \\ &\quad + \Sigma_{w=1}^{\mathfrak{q}} 32((4\mathfrak{q} - w) - 6)y^{6w+3} + \Sigma_{w=1}^{\mathfrak{q}} 32((4\mathfrak{q} - w) - 14)y^{6w+4}. \end{aligned}$$

□

Corollary 1. *The Wiener, hyper-Wiener and TSZ indices for the topology of pent–heptagonal CNS VC_5C_7 can be calculated as*

$$W(VC_5C_7) = -76 + 2774\mathfrak{q}^2 + 1960\mathfrak{q}^3 + 920\mathfrak{q}, \tag{10}$$

$$\mathrm{HW}(VC_5C_7) = \frac{1}{2}[-208 + 1471\mathfrak{q} + 8327\mathfrak{q}^2 + 14416\mathfrak{q}^3 + 7644\mathfrak{q}^4], \tag{11}$$

$$\mathrm{TSZ}(VC_5C_7) = \frac{1}{6}\left[-372 + \frac{5036}{5}\mathfrak{q} + 16128\mathfrak{q}^2 + 56732\mathfrak{q}^3 + 74520\mathfrak{q}^4 + \frac{169344}{5}\mathfrak{q}^5\right]. \tag{12}$$

Proof. The Wiener index of CNS VC_5C_7 is calculated by taking the first derivative of Hosoya polynomial at $y = 1$.

Differentiating Eq. (9) with respect to y we have

$$\frac{dH(VC_5C_7, y)}{dy} = (72\mathfrak{q} + 2) + 2(120\mathfrak{q} - 2)y + 3(152\mathfrak{q} - 6)y^2 + 4(148\mathfrak{q} - 14)y^3$$
$$+ \Sigma_{w=1}^{\mathfrak{q}} 32(6w - 1)((4\mathfrak{q} - w) + 10)y^{6w-2}$$
$$+ \Sigma_{w=1}^{\mathfrak{q}} 33(6w)((4\mathfrak{q} - w) + 6)y^{6w-1}$$
$$+ \Sigma_{w=1}^{\mathfrak{q}} 34(6w + 1)((4\mathfrak{q} - w) + 2)y^{6w}$$
$$+ \Sigma_{w=1}^{\mathfrak{q}} 33(6w + 2)((4\mathfrak{q} - w) - 2)y^{6w+1}$$
$$+ \Sigma_{w=1}^{\mathfrak{q}} 32(6w + 3)((4\mathfrak{q} - w) - 6)y^{6w+2}$$
$$+ \Sigma_{w=1}^{\mathfrak{q}} 32(6w + 4)((4\mathfrak{q} - w) - 14)y^{6w+3}.$$

Taking limit $y = 1$ gives

$$W(VC_5C_7) = \frac{dH(G, y)}{dy}|_{y=1} = (72\mathfrak{q} + 2) + 2(120\mathfrak{q} - 2)$$
$$+ 3(152\mathfrak{q} - 6) + 4(148\mathfrak{q} - 14)$$
$$+ \Sigma_{w=1}^{\mathfrak{q}} 32(6w - 1)((4\mathfrak{q} - w) + 10) + \Sigma_{w=1}^{\mathfrak{q}} 33(6w)((4\mathfrak{q} - w) + 6)$$
$$+ \Sigma_{w=1}^{\mathfrak{q}} 34(6w + 1)((4\mathfrak{q} - w) + 2) + \Sigma_{w=1}^{\mathfrak{q}} 33(6w + 2)((4\mathfrak{q} - w) - 2)$$
$$+ \Sigma_{w=1}^{\mathfrak{q}} 32(6w + 3)((4\mathfrak{q} - w) - 6) + \Sigma_{w=1}^{\mathfrak{q}} 32(6w + 4)((4\mathfrak{q} - w) - 14)$$
$$= -76 + 2774\mathfrak{q}^2 + 1960\mathfrak{q}^3 + 920\mathfrak{q}.$$

The hyper-Wiener index of CNS VC_5C_7 is calculated by multiplying Hosoya polynomial with y and then taking its second derivative at $y = 1$.

Multiplying Eq. (9) with y leads to

$$yH(VC_5C_7, y) = [(72\mathfrak{q} + 2)y^2 + (120\mathfrak{q} - 2)y^3 + (152\mathfrak{q} - 6)y^4 + (148\mathfrak{q} - 14)y^5$$
$$+ \Sigma_{w=1}^{\mathfrak{q}} 32((4\mathfrak{q} - w) + 10)y^{6w} + \Sigma_{w=1}^{\mathfrak{q}} 33((4\mathfrak{q} - w) + 6)y^{6w+1}$$
$$+ \Sigma_{w=1}^{\mathfrak{q}} 34((4\mathfrak{q} - w) + 2)y^{6w+2} + \Sigma_{w=1}^{\mathfrak{q}} 33((4\mathfrak{q} - w) - 2)y^{6w+3}$$
$$+ \Sigma_{i=1}^{\mathfrak{q}} 32((4\mathfrak{q} - w) - 6)y^{6w+4} + \Sigma_{w=1}^{\mathfrak{q}} 32((4\mathfrak{q} - w) - 14)y^{6w+5}].$$

Twice differentiation with respect to y implies the following:

$$\frac{d^2(yH(VC_5C_7, y))}{dy^2} = [2(72\mathfrak{q} + 2) + 6(120\mathfrak{q} - 2)y + 12(152\mathfrak{q} - 6)y^2$$
$$+ 20(148\mathfrak{q} - 14)y^3 + \Sigma_{w=1}^{\mathfrak{q}} (6w)(6w - 1)32$$
$$\times ((4\mathfrak{q} - w) + 10)y^{6w-2}$$
$$+ \Sigma_{w=1}^{\mathfrak{q}} (6w + 1)(6w)33((4\mathfrak{q} - w) + 6)y^{6w-1}$$

$$+ \Sigma_{w=1}^{\mathfrak{q}}(6w+2)(6w+1)34((4\mathfrak{q}-w)+2)y^{6w}$$
$$+ \Sigma_{w=1}^{\mathfrak{q}}(6w+3)(6w+2)33((4\mathfrak{q}-w)-2)y^{6w+1}$$
$$+ \Sigma_{w=1}^{\mathfrak{q}}(6w+4)(6w+3)32((4\mathfrak{q}-w)-6)y^{6w+2}$$
$$+ \Sigma_{w=1}^{\mathfrak{q}}(6w+5)(6w+4)32((4\mathfrak{q}-w)-14)y^{6w+3}].$$

Taking limit at $y = 1$ gives

$$\begin{aligned}
\mathrm{HW}(VC_5C_7) = \frac{d^2(yH(G,y))}{dy^2}|_{y=1} &= [2(72\mathfrak{q}+2) + 6(120\mathfrak{q}-2) + 12(152\mathfrak{q}-6) \\
&+ 20(148\mathfrak{q}-14) + \Sigma_{w=1}^{\mathfrak{q}}(6w)(6w-1)32((4\mathfrak{q}-w)+10) \\
&+ \Sigma_{w=1}^{\mathfrak{q}}(6w+1)(6w)33((4\mathfrak{q}-w)+6) \\
&+ \Sigma_{w=1}^{\mathfrak{q}}(6w+2)(6w+1)34((4\mathfrak{q}-w)+2) \\
&+ \Sigma_{w=1}^{\mathfrak{q}}(6w+3)(6w+2)33((4\mathfrak{q}-w)-2) \\
&+ \Sigma_{w=1}^{\mathfrak{q}}(6w+4)(6w+3)32((4\mathfrak{q}-w)-6) \\
&+ \Sigma_{w=1}^{\mathfrak{q}}(6w+5)(6w+4)32((4\mathfrak{q}-w)-14)], \\
&= \frac{1}{2}[-208 + 1471\mathfrak{q} + 8327\mathfrak{q}^2 + 14416\mathfrak{q}^3 + 7644\mathfrak{q}^4].
\end{aligned}$$

The TSZ index of CNS HC_5C_7 is calculated by multiplying Hosoya polynomial by y^2 and then taking the third derivative at $y = 1$. Multiply Eq. (9) with y^2 gives

$$\begin{aligned}
y^2H(VC_5C_7, y) &= (72\mathfrak{q}+2)y^3 + (120\mathfrak{q}-2)y^4 + (152\mathfrak{q}-6)y^5 + (148\mathfrak{q}-14)y^6 \\
&+ \Sigma_{w=1}^{\mathfrak{q}}32((4\mathfrak{q}-w)+10)y^{6w+1} + \Sigma_{w=1}^{\mathfrak{q}}33((4\mathfrak{q}-w)+6)y^{6w+2} \\
&+ \Sigma_{w=1}^{\mathfrak{q}}34((4\mathfrak{q}-w)+2)y^{6w+3} + \Sigma_{w=1}^{\mathfrak{q}}33((4\mathfrak{q}-w)-2)y^{6w+4} \\
&+ \Sigma_{w=1}^{\mathfrak{q}}32((4\mathfrak{q}-w)-6)y^{6w+5} + \Sigma_{w=1}^{\mathfrak{q}}32((4\mathfrak{q}-w)-14)y^{6w+6}.
\end{aligned}$$

Taking third derivative with respect to y gives

$$\begin{aligned}
\frac{d^3(y^2H(G,y))}{dy^3} &= 6(72n\mathfrak{q}+2) + 24(120\mathfrak{q}-2)y + 60(152\mathfrak{q}-6)y^2 + 120(148\mathfrak{q}-14)y^3 \\
&+ \Sigma_{w=1}^{\mathfrak{q}}(6w+1)(6w)(6w-1)32((4\mathfrak{q}-w)+10)y^{6w-2} \\
&+ \Sigma_{w=1}^{\mathfrak{q}}(6w+2)(6w+1)(6w)33((4\mathfrak{q}-w)+6)y^{6w-1} \\
&+ \Sigma_{w=1}^{\mathfrak{q}}(6w+3)(6w+2)(6w+1)34((4\mathfrak{q}-w)+2)y^{6w} \\
&+ \Sigma_{w=1}^{\mathfrak{q}}(6w+4)(6w+3)(6w+2)33((4\mathfrak{q}-w)-2)y^{6w+1} \\
&+ \Sigma_{w=1}^{\mathfrak{q}}(6w+5)(6w+4)(6w+3)32((4\mathfrak{q}-w)-6)y^{6w+2} \\
&+ \Sigma_{w=1}^{\mathfrak{q}}(6w+6)(6w+5)(6w+4)32((4\mathfrak{q}-w)-14)y^{6w+3}.
\end{aligned}$$

Taking limit $y = 1$ implies

$$\begin{aligned}
\mathrm{TSZ}(VC_5C_7) &= \frac{d^3(y^2H(G,y))}{dy^3}|_{y=1} = 6(72\mathfrak{q}+2) + 24(120\mathfrak{q}-2) + 60(152\mathfrak{q}-6) \\
&\quad + 120(148\mathfrak{q}-14) + \Sigma_{w=1}^{\mathfrak{q}}(6w+1)(6w)(6w-1)32((4\mathfrak{q}-w)+10) \\
&\quad + \Sigma_{w=1}^{\mathfrak{q}}(6w+2)(6w+1)(6w)33((4\mathfrak{q}-w)+6) \\
&\quad + \Sigma_{w=1}^{\mathfrak{q}}(6w+3)(6w+2)(6w+1)34((4\mathfrak{q}-w)+2) \\
&\quad + \Sigma_{w=1}^{\mathfrak{q}}(6w+4)(6w+3)(6w+2)33((4\mathfrak{q}-w)-2) \\
&\quad + \Sigma_{w=1}^{\mathfrak{q}}(6w+5)(6w+4)(6w+3)32((4\mathfrak{q}-w)-6) \\
&\quad + \Sigma_{w=1}^{\mathfrak{q}}(6w+6)(6w+5)(6w+4)32((4\mathfrak{q}-w)-14) \\
&= \frac{1}{6}\left[-372 + \frac{5036}{5}\mathfrak{q} + 16128\mathfrak{q}^2 + 56732\mathfrak{q}^3 + 74520\mathfrak{q}^4 + \frac{169344}{5}\mathfrak{q}^5\right].
\end{aligned}$$

□

3.2. *Pent–heptagonal CNS HC_5C_7*

A HC_5C_7 is the horizontal arrangement of CNS C_5C_7. Thus, a two-dimensional lattice is developed which entertain C_5 as pentagon and C_7 as heptagon in HC_5C_7 is shown in Fig. 2. It is noteworthy that in the arrangement $HC_5C_7[n]$, $n > 1$ is the length of the sheet.

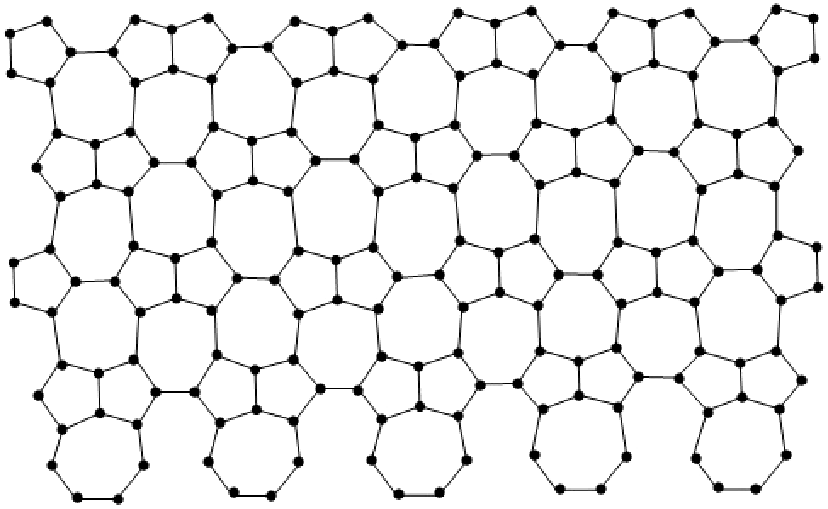

Fig. 2. The molecular graph of CNS HC_5C_7.

Theorem 2. *For the topology of pent–heptagonal CNS HC_4C_8, the Hosoya polynomial is calculated as*

$$\begin{aligned} H(HC_5C_7, y) = {} & (20\mathfrak{q}+2)y + (32\mathfrak{q}-2)y^2 + (28\mathfrak{q}-6)y^3 \\ & + \Sigma_{w=1}^{\mathfrak{q}}(13(2\mathfrak{q}-w)-8)y^{5w-1} \\ & + \Sigma_{w=1}^{\mathfrak{q}}(14(2\mathfrak{q}-w)+4)y^{5w} + \Sigma_{w=1}^{\mathfrak{q}}(13(2\mathfrak{q}-w))y^{5w+1} \\ & + \Sigma_{w=1}^{\mathfrak{q}}(12(2\mathfrak{q}-w)-4)y^{5w+2} + \Sigma_{w=1}^{\mathfrak{q}}(12(2\mathfrak{q}-w)-4)y^{5w+3}. \end{aligned} \quad (13)$$

Proof. The distance matrix D corresponding to the molecular graph of CNS HC_5C_7 is

$$D = \begin{bmatrix} A_0 & A_1 & A_2 & A_3 & A_4 & A_5 & \dots & A_{2\mathfrak{q}} & C_{2\mathfrak{q}+1} \\ A_1^T & A_0 & A_1 & A_2 & A_3 & A_4 & \dots & A_{2\mathfrak{q}-1} & C_{2\mathfrak{q}} \\ A_2^T & A_1^T & A_0 & A_1 & A_2 & A_3 & \dots & A_{2\mathfrak{q}-2} & C_{2\mathfrak{q}-1} \\ A_3^T & A_2^T & A_1^T & A_0 & A_1 & A_2 & \dots & A_{2\mathfrak{q}-3} & C_{2\mathfrak{q}-2} \\ A_4^T & A_3^T & A_2^T & A_1^T & A_0 & A_1 & \dots & A_{2\mathfrak{q}-4} & C_{2\mathfrak{q}-3} \\ A_5^T & A_4^T & A_3^T & A_2^T & A_1^T & A_o & \dots & A_{2\mathfrak{q}-5} & C_{2\mathfrak{q}-4} \\ . & . & . & . & . & . & . & . & \\ . & . & . & . & . & . & . & . & \\ . & . & . & . & . & . & . & . & \\ A_{2\mathfrak{q}}^T & A_{2\mathfrak{q}-1}^T & A_{2\mathfrak{q}-2}^T & A_{2\mathfrak{q}-3}^T & A_{2\mathfrak{q}-4}^T & A_{2\mathfrak{q}-5}^T & \dots & A_0 & C_1 \\ C_{2\mathfrak{q}+1}^T & C_{2\mathfrak{q}}^T & C_{2\mathfrak{q}-1}^T & C_{2\mathfrak{q}-2}^T & C_{2\mathfrak{q}-3}^T & C_{2\mathfrak{q}-4}^T & \dots & C_1^T & C_0 \end{bmatrix},$$

where $A_0, A_1, A_2, A_3, A_4, A_5, \dots, A_{2\mathfrak{q}}$ and $C_0, C_1, C_2, C_3, C_4, C_5, \dots, C_{2\mathfrak{q}+1}$ are the submatrices. These matrices can be computed as follows ($\spadesuit = 5\mathfrak{q}$):

$$A_0 = \begin{bmatrix} 0 & 1 & 1 & 2 & 2 & 3 & 4 & 4 \\ 1 & 0 & 2 & 1 & 2 & 3 & 4 & 4 \\ 1 & 2 & 0 & 2 & 1 & 2 & 3 & 3 \\ 2 & 1 & 2 & 0 & 1 & 2 & 3 & 3 \\ 2 & 2 & 1 & 1 & 0 & 1 & 2 & 2 \\ 3 & 3 & 2 & 2 & 1 & 0 & 1 & 1 \\ 4 & 4 & 3 & 3 & 2 & 1 & 0 & 2 \\ 4 & 4 & 3 & 3 & 2 & 1 & 2 & 0 \end{bmatrix}, \quad A_1 = \begin{bmatrix} 5 & 5 & 6 & 6 & 7 & 8 & 9 & 9 \\ 5 & 5 & 6 & 6 & 7 & 8 & 9 & 9 \\ 4 & 4 & 5 & 5 & 6 & 7 & 8 & 8 \\ 4 & 4 & 5 & 5 & 6 & 7 & 8 & 8 \\ 3 & 3 & 4 & 4 & 5 & 6 & 7 & 7 \\ 2 & 2 & 3 & 3 & 4 & 5 & 6 & 6 \\ 1 & 2 & 2 & 2 & 3 & 4 & 5 & 5 \\ 2 & 1 & 3 & 3 & 3 & 4 & 5 & 5 \end{bmatrix},$$

$$A_k = \begin{bmatrix} \spadesuit+5 & \spadesuit+5 & \spadesuit+6 & \spadesuit+6 & \spadesuit+7 & \spadesuit+8 & \spadesuit+9 & \spadesuit+9 \\ \spadesuit+5 & \spadesuit+5 & \spadesuit+6 & \spadesuit+6 & \spadesuit+7 & \spadesuit+8 & \spadesuit+9 & \spadesuit+9 \\ \spadesuit+4 & \spadesuit+4 & \spadesuit+5 & \spadesuit+5 & \spadesuit+6 & \spadesuit+7 & \spadesuit+8 & \spadesuit+8 \\ \spadesuit+4 & \spadesuit+4 & \spadesuit+5 & \spadesuit+5 & \spadesuit+6 & \spadesuit+7 & \spadesuit+8 & \spadesuit+8 \\ \spadesuit+3 & \spadesuit+3 & \spadesuit+4 & \spadesuit+4 & \spadesuit+5 & \spadesuit+6 & \spadesuit+7 & \spadesuit+7 \\ \spadesuit+2 & \spadesuit+2 & \spadesuit+3 & \spadesuit+3 & \spadesuit+4 & \spadesuit+5 & \spadesuit+6 & \spadesuit+6 \\ \spadesuit+1 & \spadesuit+1 & \spadesuit+2 & \spadesuit+2 & \spadesuit+3 & \spadesuit+4 & \spadesuit+5 & \spadesuit+5 \\ \spadesuit+1 & \spadesuit+1 & \spadesuit+2 & \spadesuit+2 & \spadesuit+3 & \spadesuit+4 & \spadesuit+5 & \spadesuit+5 \end{bmatrix}_{1\le k\le 2\mathfrak{q}},$$

$$C_0 = \begin{bmatrix} 0 & 1 \\ 1 & 0 \end{bmatrix}, \quad C_1 = \begin{bmatrix} 5 & 5 \\ 5 & 5 \\ 4 & 4 \\ 4 & 4 \\ 3 & 3 \\ 2 & 2 \\ 1 & 2 \\ 2 & 1 \end{bmatrix}, \quad C_k = \begin{bmatrix} \spadesuit+5 & \spadesuit+5 \\ \spadesuit+5 & \spadesuit+5 \\ \spadesuit+4 & \spadesuit+4 \\ \spadesuit+4 & \spadesuit+4 \\ \spadesuit+3 & \spadesuit+3 \\ \spadesuit+2 & \spadesuit+2 \\ \spadesuit+1 & \spadesuit+1 \\ \spadesuit+1 & \spadesuit+1 \end{bmatrix}_{1\le k\le 2\mathfrak{q}+1}.$$

For the sake of computing $|l_k(\mathfrak{q})|$ (k is the distance between the pairs), we can calculate as follows:

$$\begin{aligned} l_1(n) &= [\#1 \in A_0] \times [\#A_0] + [\#1 \in A_1] \times [\#A_1] + [\#1 \in C_0] \times [\#C_0] \\ &\quad + [\#1 \in C_1] \times [\#C_1] \\ &= 8(2\mathfrak{q}) + 2(2\mathfrak{q}-1) + 2(1) + 2(1) \\ &= 16\mathfrak{q} + 4\mathfrak{q} - 2 + 2 + 2 \\ &= 20\mathfrak{q} + 2. \end{aligned}$$

Similarly,

$$\begin{aligned} |l_2(\mathfrak{q})| &= 32n - 2, \quad |l_3(\mathfrak{q})| = 28\mathfrak{q} - 6, \\ |l_{5w-1}(\mathfrak{q})| &= \Sigma_{w=1}^{\mathfrak{q}} 13(2\mathfrak{q} - w) - 8, \quad |l_{5w}(\mathfrak{q})| = \Sigma_{w=1}^{\mathfrak{q}} 14(2\mathfrak{q} - w) + 4, \\ |l_{5w+1}(\mathfrak{q})| &= \Sigma_{w=1}^{\mathfrak{q}} 13(2\mathfrak{q} - w), \quad |l_{5w+2}(\mathfrak{q})| = \Sigma_{w=1}^{\mathfrak{q}} 12(2\mathfrak{q} - w) - 4, \\ |l_{5w+3}(\mathfrak{q})| &= \Sigma_{w=1}^{\mathfrak{q}} 12(2\mathfrak{q} - w) - 4. \end{aligned}$$

Substituting these values into Eq. (5) lead to the following form of Hosoya polynomial for pent–heptagonal CNS HC_5C_7 as

$$\begin{aligned}H(HC_5C_7, y) = {} & (20\mathfrak{q}+2)y + (32\mathfrak{q}-2)y^2 + (28\mathfrak{q}-6)y^3 \\ & + \Sigma_{w=1}^{\mathfrak{q}}(13(2\mathfrak{q}-w)-8)y^{5w-1} \\ & + \Sigma_{w=1}^{\mathfrak{q}}(14(2\mathfrak{q}-w)+4)y^{5w} + \Sigma_{w=1}^{\mathfrak{q}}(13(2\mathfrak{q}-w))y^{5w+1} \\ & + \Sigma_{w=1}^{\mathfrak{q}}(12(2\mathfrak{q}-w)-4)y^{5w+2} + \Sigma_{w=1}^{\mathfrak{q}}(12(2\mathfrak{q}-w)-4)y^{5w+3}.\end{aligned}$$

□

Corollary 2. *The Wiener, hyper-Wiener and TSZ indices for the topology of pent–heptagonal CNS HC_5C_7 can be calculated as*

$$W(HC_5C_7) = -20 + \frac{158}{3}\mathfrak{q} + 202\mathfrak{q}^2 + \frac{640}{3}\mathfrak{q}^3, \tag{14}$$

$$\mathrm{HW}(HC_5C_7) = \frac{1}{2}\left[-40 + \frac{229}{3}\mathfrak{q} + \frac{493}{3}\mathfrak{q}^2 + \frac{2420}{3}\mathfrak{q}^3 + \frac{2000}{3}\mathfrak{q}^4\right], \tag{15}$$

$$\mathrm{TSZ}(HC_5C_7) = \frac{1}{6}[-36 + 160\mathfrak{q} - 167\mathfrak{q}^2 + 770\mathfrak{q}^3 + 3125\mathfrak{q}^4 + 2400\mathfrak{q}^5]. \tag{16}$$

Proof. The Wiener index of CNS HC_5C_7 is calculated by taking the first derivative of Hosoya polynomial at $y = 1$.

Differentiating Eq. (13) with respect to y we have

$$\begin{aligned}\frac{dH(HC_5C_7, y)}{dy} = {} & (20\mathfrak{q}+2) + 2(32\mathfrak{q}-2)y + 3(28\mathfrak{q}-6)y^2 \\ & + \Sigma_{w=1}^{\mathfrak{q}}(5w-1)(13(2\mathfrak{q}-w)-8)y^{5w-2} \\ & + \Sigma_{w=1}^{\mathfrak{q}}(5w)(14(2\mathfrak{q}-w)+4)y^{5w-1} \\ & + \Sigma_{w=1}^{\mathfrak{q}}(5w+1)(13(2\mathfrak{q}-w))y^{5w} \\ & + \Sigma_{w=1}^{\mathfrak{q}}(5w+2)(12(2\mathfrak{q}-w)-4)y^{5w+1} \\ & + \Sigma_{w=1}^{\mathfrak{q}}(5w+3)(12(2\mathfrak{q}-w)-4)y^{5w+2}.\end{aligned}$$

Taking limit $y = 1$ gives

$$\begin{aligned}W(HC_5C_7) = {} & \frac{dH(HC_5C_7, y)}{dy}\Big|_{y=1} = (20\mathfrak{q}+2) + 2(32\mathfrak{q}-2) + 3(28\mathfrak{q}-6) \\ & + \Sigma_{w=1}^{\mathfrak{q}}(5w-1)(13(2\mathfrak{q}-w)-8) + \Sigma_{w=1}^{\mathfrak{q}}(5w)(14(2\mathfrak{q}-w)+4) \\ & + \Sigma_{w=1}^{\mathfrak{q}}(5w+1)(13(2\mathfrak{q}-w)) + \Sigma_{w=1}^{\mathfrak{q}}(5w+2)(12(2\mathfrak{q}-w)-4) \\ & + \Sigma_{w=1}^{\mathfrak{q}}(5w+3)(12(2\mathfrak{q}-w)-4) \\ = {} & -20 + \frac{158}{3}\mathfrak{q} + 202\mathfrak{q}^2 + \frac{640}{3}\mathfrak{q}^3.\end{aligned}$$

The hyper-Wiener index of CNS HC_5C_7 is calculated by multiplying Hosoya polynomial with y and then taking its second derivative at $y = 1$.

Multiplying Eq. (13) with y leads to

$$\begin{aligned} yH(HC_5C_7, y) &= (20\mathfrak{q} + 2)y^2 + (32\mathfrak{q} - 2)y^3 + (28\mathfrak{q} - 6)y^4 \\ &\quad + \Sigma_{w=1}^{\mathfrak{q}}(13(2\mathfrak{q} - w) - 8)y^{5w} + \Sigma_{w=1}^{\mathfrak{q}}(14(2\mathfrak{q} - w) + 4)y^{5w+1} \\ &\quad + \Sigma_{w=1}^{\mathfrak{q}}(13(2\mathfrak{q} - w))y^{5w+2} + \Sigma_{w=1}^{\mathfrak{q}}(12(2\mathfrak{q} - w) - 4)y^{5w+3} \\ &\quad + \Sigma_{w=1}^{\mathfrak{q}}(12(2\mathfrak{q} - w) - 4)y^{5w+4}. \end{aligned}$$

Twice differentiation with respect to y implies

$$\begin{aligned} \frac{d^2yH(G, y)}{dy^2} &= 2(20\mathfrak{q} + 2) + 6(32\mathfrak{q} - 2)y + 12(28\mathfrak{q} - 6)y^2 \\ &\quad + \Sigma_{w=1}^{\mathfrak{q}}(5w)(5w - 1)(13(2\mathfrak{q} - w) - 8)y^{5w-2} \\ &\quad + \Sigma_{w=1}^{\mathfrak{q}}(5w + 1)(5w)(14(2\mathfrak{q} - w) + 4)y^{5w-1} \\ &\quad + \Sigma_{w=1}^{\mathfrak{q}}(5w + 2)(5w + 1)(13(2\mathfrak{q} - w))y^{5w} \\ &\quad + \Sigma_{w=1}^{\mathfrak{q}}(5w + 3)(5w + 2)(12(2\mathfrak{q} - w) - 4)y^{5w+1} \\ &\quad + \Sigma_{w=1}^{\mathfrak{q}}(5w + 4)(5w + 3)(12(2\mathfrak{q} - w) - 4)y^{5w+2}. \end{aligned}$$

Taking limit at $y = 1$ gives

$$\begin{aligned} \mathrm{HW}(HC_5C_7) &= \frac{d^2yH(HC_5C_7, y)}{dy^2} = 2(20\mathfrak{q} + 2) + 6(32\mathfrak{q} - 2) + 12(28\mathfrak{q} - 6) \\ &\quad + \Sigma_{w=1}^{\mathfrak{q}}(5w)(5w - 1)(13(2\mathfrak{q} - w) - 8) \\ &\quad + \Sigma_{w=1}^{\mathfrak{q}}(5w + 1)(5w)(14(2\mathfrak{q} - w) + 4) \\ &\quad + \Sigma_{w=1}^{\mathfrak{q}}(5w + 2)(5w + 1)(13(2\mathfrak{q} - w)) \\ &\quad + \Sigma_{w=1}^{\mathfrak{q}}(5w + 3)(5w + 2)(12(2\mathfrak{q} - w) - 4) \\ &\quad + \Sigma_{w=1}^{\mathfrak{q}}(5w + 4)(5w + 3)(12(2\mathfrak{q} - w) - 4) \\ &= \frac{1}{2}\left[-40 + \frac{229}{3}\mathfrak{q} + \frac{493}{3}\mathfrak{q}^2 + \frac{2420}{3}\mathfrak{q}^3 + \frac{2000}{3}\mathfrak{q}^4\right]. \end{aligned}$$

The TSZ index of CNS HC_5C_7 is calculated by multiplying Hosoya polynomial by y^2 and then taking the third derivative at $y = 1$.

Multiply Eq. (13) with y^2 gives

$$\begin{aligned} y^2H(HC_5C_7, y) &= (20\mathfrak{q} + 2)y^3 + (32\mathfrak{q} - 2)y^4 + (28\mathfrak{q} - 6)y^5 \\ &\quad + \Sigma_{w=1}^{\mathfrak{q}}(13(2\mathfrak{q} - w) - 8)y^{5w+1} \end{aligned}$$

$$
\begin{aligned}
&+\Sigma_{w=1}^{\mathfrak{q}}(14(2\mathfrak{q}-w)+4)y^{5w+2}\\
&+\Sigma_{w=1}^{\mathfrak{q}}(13(2\mathfrak{q}-w))y^{5w+3}\\
&+\Sigma_{w=1}^{\mathfrak{q}}(12(2\mathfrak{q}-w)-4)y^{5w+4}\\
&+\Sigma_{w=1}^{\mathfrak{q}}(12(2\mathfrak{q}-w)-4)y^{5w+5}.
\end{aligned}
$$

Taking third derivative with respect to y gives

$$
\begin{aligned}
\frac{d^3y^2H(G,y)}{dy^3} &= 6(20\mathfrak{q}+2)+24(32\mathfrak{q}-2)y+60(28\mathfrak{q}-6)y^2\\
&+\Sigma_{w=1}^{\mathfrak{q}}(5w+1)(5w)(5w-1)(13(2\mathfrak{q}-w)-8)y^{5w-2}\\
&+\Sigma_{w=1}^{\mathfrak{q}}(5w+2)(5w+1)(5w)(14(2\mathfrak{q}-w)+4)y^{5w-1}\\
&+\Sigma_{w=1}^{\mathfrak{q}}(5w+3)(5w+2)(5w+1)(13(2\mathfrak{q}-w))y^{5w}\\
&+\Sigma_{w=1}^{\mathfrak{q}}(5w+4)(5w+3)(5w+2)(12(2\mathfrak{q}-w)-4)y^{5w+1}\\
&+\Sigma_{w=1}^{\mathfrak{q}}(5w+5)(5w+4)(5w+3)(12(2\mathfrak{q}-w)-4)y^{5w+2}.
\end{aligned}
$$

Taking limit $y=1$ implies

$$
\begin{aligned}
\mathrm{TSZ}(HC_5C_7) &= \frac{d^3y^2H(G,y)}{dy^3}|_{y=1} = 6(20\mathfrak{q}+2)+24(32\mathfrak{q}-2)+60(28\mathfrak{q}-6)\\
&+\Sigma_{w=1}^{\mathfrak{q}}(5w+1)(5w)(5w-1)(13(2\mathfrak{q}-w)-8)\\
&+\Sigma_{w=1}^{\mathfrak{q}}(5w+2)(5w+1)(5w)(14(2\mathfrak{q}-w)+4)\\
&+\Sigma_{w=1}^{\mathfrak{q}}(5w+3)(5w+2)(5w+1)(13(2\mathfrak{q}-w))\\
&+\Sigma_{w=1}^{\mathfrak{q}}(5w+4)(5w+3)(5w+2)(12(2\mathfrak{q}-w)-4)\\
&+\Sigma_{w=1}^{\mathfrak{q}}(5w+5)(5w+4)(5w+3)(12(2\mathfrak{q}-w)-4),\\
&= \frac{1}{6}[-36+160\mathfrak{q}-167\mathfrak{q}^2+770\mathfrak{q}^3+3125\mathfrak{q}^4+2400\mathfrak{q}^5]. \qquad \square
\end{aligned}
$$

4. Discussion

We have calculated Hosoya polynomial and its subsequent topological indices including Wiener, hyper-Wiener and TSZ indices for VC_5C_7 and HC_5C_7 CNS. It is found that both the sheets have same chemical formula but different molecular configuration leads to different Hosoya polynomial. Moreover, these Hosoya polynomials lead to distance base polynomials including Wiener, hyper-Wiener and TSZ indices. We have obtained these indices which are found to be different for the two CNS. The graphs of these indices are given as follows:

Figures 3 and 4 depict the Wiener, hyper-Wiener and TSZ indices for VC_5C_7 and HC_5C_7 CNS, respectively. These indices are exhibit for $\mathfrak{q}\epsilon[1,5]$. Both the figures indicate that all the three indices possess different values for the two CNS. Moreover,

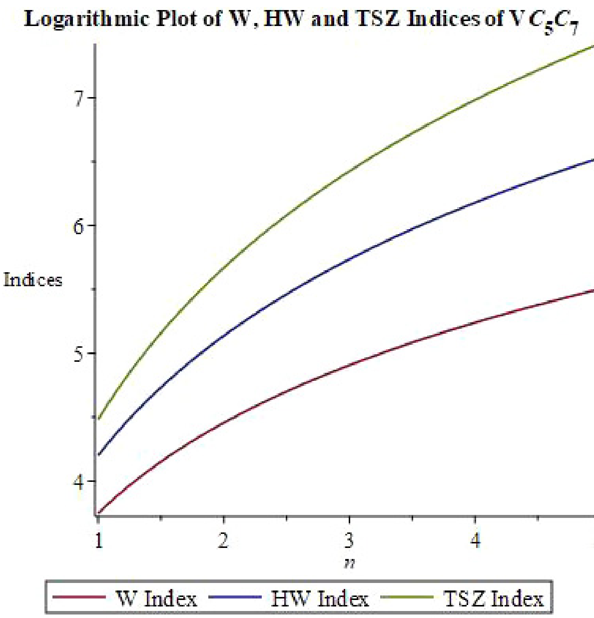

Fig. 3. Wiener, hyper-Wiener and TSZ indices of VC_5C_7.

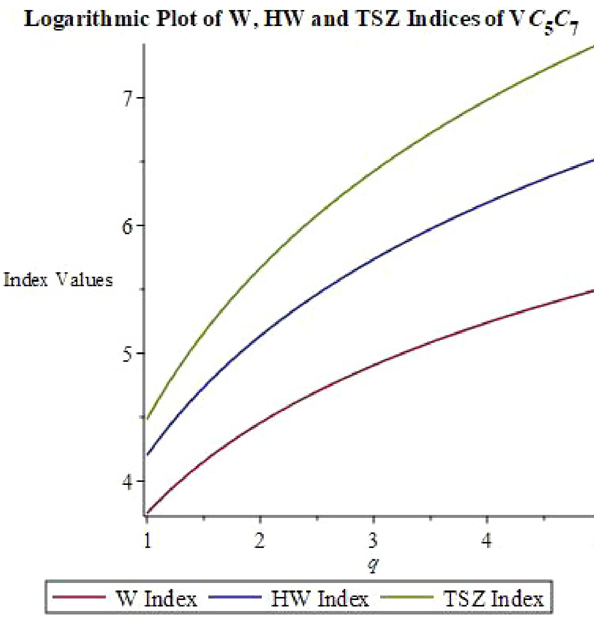

Fig. 4. Wiener, hyper-Wiener and TSZ indices of HC_5C_7.

the values of all the indices are increasing with the increase in $\mathfrak{q}$. It is interesting to note that these indices posses physical and reliable values at only discrete $\mathfrak{q}$, i.e. $\mathfrak{q} = 1, 2, 3, 4, 5$. The Wiener index possesses the lesser value as compared to the other two indices. The hyper-Wiener index admits greater values as compared to those of Weiner index. The TSZ index carries the greatest values as compared to Wiener and hyper-Wiener indices.

5. Conclusion

This paper is devoted to the calculation of the Hosoya polynomial and its subsequent topological indices for the topology of pent–heptagonal CNS VC_5C_7 and HC_5C_7. The Hosoya polynomial is the closed form of the Wiener, hyper-Wiener and TSZ indices. There are several physical applications for these indices. These Hosoya polynomial derivatives, for instance, address a molecule's surface area and branching. Additionally, they are connected to formation heat, melting points, density, boiling temperatures, critical points, vaporization, cyclicity, aromatic hydrocarbon saturation, alkane and alcohol ultrasonic velocities, electroreduction and carbonization. These characteristics make these indices effective for developing new medications [29, 38]. The sub-atomic stretching in electronic structures is also presented using these indices. These indices are used to increase the hardware security of the computer network lattice. They also offer the physio-chemical characteristics of organic compounds in pharmacology [39].

It is noteworthy that both the pent–heptagonal CNS structures, VC_5C_7 and HC_5C_7 of the same atomic structure C_5C_7 nanosheet reached at two different Hosoya polynomials. As a consequence, the related distance-based topological indices including Wiener, hyper-Wiener and TSZ indices of both the pent–heptagonal CNS structures (VC_5C_7 and HC_5C_7) are different. The graphical analysis of these indices for the two CNS depicts that the Wiener index possesses lesser values, the hyper-Wiener admits relatively greater values whereas the TSZ index takes the greatest values for all n. This leads to different QSPR and QSAR for both the CNS.

Acknowledgments

This work was partially funded by Slovak Grant Agency for Science VEGA under the grant number VEGA 2/0009/19. Moreover, the authors acknowledge the support of HEC Pakistan, University of Education, Lahore and National Textile University, Faisalabad for their administrative and technical support.

References

[1] A. Singh and D. K. Patel, Nanomaterials for biomedical engineering applications, in *Nanomaterials for Advanced Technologies* (Springer, Singapore, 2022), pp. 75–102.

[2] M. Zain, H. Yasmeen, S. S. Yadav, S. Amir, M. Bilal, A. Shahid and M. Khurshid, Applications of nanotechnology in biological systems and medicine, in *Nanotechnology*

for Hematology, Blood Transfusion, and Artificial Blood (Elsevier, 2022), pp. 215–235.
[3] J. Xu, Y. Jiang, X. Chen, Z. Tang, Y. Gao, M. Huang, Y. Wan, P. Cheng and G. Wang, Photo-and magneto-responsive highly graphitized carbon based phase change composites for energy conversion and storage, *Mater. Today Nano* **19** (2022) 100234.
[4] M. R. Alam, T. Islam, M. R. Repon and M. E. Hoque, Carbon-based polymer nanocomposites for electronic textiles (e-textiles), in *Advanced Polymer Nanocomposites* (Woodhead Publishing, 2022), pp. 443–482.
[5] R. Eivazzadeh-Keihan, E. B. Noruzi, E. Chidar, M. Jafari, F. Davoodi, A. Kashtiaray, M. G. Gorab, S. M. Hashemi, S. Javanshir, R. A. Cohan, A. Maleki and M. Mahdavi, Applications of carbon-based conductive nanomaterials in biosensors, *J. Chem. Eng.* **442**(Part 1) (2022) 136183.
[6] C. T. Nottbohm, Carbon nanosheets and their applications, dissertation, Bielefeld University, Bielefeld, Germany (2009).
[7] J. Guo, J. Zhang, F. Jiang, S. Zhao, Q. Su and G. Du, Microporous carbon nanosheets derived from corncobs for lithium sulfur batteries, *Electrochim. Acta* **176** (2015) 853–860.
[8] M. Sevilla and A. B. Fuertes, Direct synthesis of highly porous interconnected carbon nanosheets and their application as high-performance supercapacitors, *ACS Nano* **8**(5) (2014) 5069–5078.
[9] W. Wei, H. Liang, K. Parvez, X. Zhuang, X. Feng and K. Mãllen, Nitrogen-doped carbon nanosheets with size-defined mesopores as highly efficient metal-free catalyst for the oxygen reduction reaction, *Angew. Chem.* **126**(6) (2014) 1596–1600.
[10] A. Mahto, A. Singh, K. Aruchamy, A. Maraddi, G. R. Bhadu, N. S. Kotrappanavar and R. Meena, A hyperaccumulation pathway to hierarchically porous carbon nanosheets from halophyte biomass for wastewater remediation, *Sustain. Mater. Technol.* **29** (2021) e00292.
[11] C. Cheng, S. He, C. Zhang, C. Du and W. Chen, High-performance supercapacitor fabricated from 3D free-standing hierarchical carbon foam-supported two dimensional porous thin carbon nanosheets, *Electrochim. Acta* **290** (2018) 98–108.
[12] C. Zhu, H. Li, S. Fu, D. Duab and Y. Lin, Highly efficient nonprecious metal catalysts towards oxygen reduction reaction based on three-dimensional porous carbon nanostructures, *Chem. Soc. Rev.* **45**(3) (2016) 517–531.
[13] H. Wiener, Structural determination of paraffin boiling points, *J. Amer. Chem. Soc.* **69** (1947) 17–20.
[14] M. Adnan, S. A. Bokhary, G. Abbas and T. Iqbal, Degree-based topological indices and QSPR analysis of antituberculosis drugs, *J. Chem.* **2022** (2022) 574862.
[15] M. Randić, Novel molecular descriptor for structure–property studies, *Chem. Phys. Lett.* **211** (1993) 478–483.
[16] Á. Martínez-Pérez and J. M. Rodríguez, New bounds for topological indices on trees through generalized methods, *Symmetry* **12**(7) (2020) 12071097.
[17] S. S. Tratch, M. I. Stankevitch and N. S. Zefirov, Combinatorial models and algorithms in chemistry. The expanded Wiener number — A novel topological index, *J. Comput. Chem.* **11**(8) (1990) 899–908.
[18] H. Hosoya, On some counting polynomials in chemistry, *Discrete Appl. Math.* **19**(1–3) (1988) 239–257.
[19] I. Gutman, S. Klavžar, M. Petkovšek and P. Žigert, On Hosoya polynomial of benzenoid graphs, *MATCH Commun. Math. Comput. Chem.* **43** (2001) 49–66.
[20] G. Cash, Relationship between the Hosoya polynomial and the hyper-Wiener index, *Appl. Math. Lett.* **15**(7) (2002) 893–895.

[21] D. M. Joita and L. Jantschi, Extending the characteristic polynomial for characterization of C_{20} fullerene congeners, *Mathematics* **5**(4) (2017) 84.
[22] M. Z. Gecmen and E. Celik, Numerical solution of Volterra–Fredholm integral equations with Hosoya polynomials, *Math. Methods Appl. Sci.* **44**(14) (2021) 11166–11173.
[23] L. Chen, A. Mehboob, H. Ahmad, W. Nazeer, M. Hussain and M. R. Farahani, Hosoya and Harary polynomials of TOX(n), RTOX(n), TSL(n) and RTSL(n), *Discrete Dyn. Nat. Soc.* **2019** (2019) 8696982.
[24] A. R. Nizami, K. Shabbir, M. S. Sardar, M. Qasim, M. Cancan and S. Ediz, Base polynomials for degree and distance based topological invariants of n-bilinear straight pentachain, *J. Optim. Theory Appl.* **42**(7) (2021) 1479–1495.
[25] X. Lin, X. Guo and X. Chen, A general formula for computing the Hosoya polynomial of capped armchair nanotubes, *Polycycl. Aromat. Compd.* **41**(5) (2021) 907–919.
[26] D. Wang, H. Ahmad and W. Nazeer, Hosoya and Harary polynomials of TUC_4 nanotube, *Math. Methods Appl. Sci.* (2020) 1–17.
[27] U. Sheikh, S. Rashid, C. Ozel and R. Pincak, On Hosoya polynomial and subsequent indices of $C_4C_8(R)$ and $C_4C_8(S)$ nanosheets, *Symmetry* **14**(7) (2022) 1349.
[28] A. M. Ali, H. O. Abdullah and G. A. M. Saleh, Hosoya polynomials and Wiener indices of carbon nanotubes using mathematica programming, *J. Discrete Math. Sci. Cryptogr.* **25**(1) (2022) 147–158.
[29] Z. B. Peng, A. R. Nizami, Z. Iqbal, M. M. Munir, H. M. W. Ahmed and J. B. Liu, Wiener and hyper-Wiener indices of polygonal cylinder and torus, *Complexity* **2021** (2021) 8882646.
[30] M. Arockiaraw, S. Klavžar, S. Mushtaq and K. Balasubramanian, Distance-based topological indices of nanosheets, nanotubes and nanotori of SiO_2, *J. Math. Chem.* **57** (2019) 343–369.
[31] S. Mondal, N. De and A. Pal, Topological indices of some chemical structures applied for the treatment of COVID-19 patients, *Polycycl. Aromat. Compd.* **42**(4) (2022) 1220–1234.
[32] S. A. K. Kirmani, P. Ali and F. Azam, Topological indices and QSPR/QSAR analysis of some antiviral drugs being investigated for the treatment of COVID-19 patients, *Int. J. Quantum Chem.* **121**(9) (2021) e26594.
[33] J. B. Liu, M. Arockiaraj, M. Arulperumjothi and S. Prabhu, Distance based and bond additive topological indices of certain repurposed antiviral drug compounds tested for treating COVID-19, *Int. J. Quantum Chem.* **121**(10) (2021) e26617.
[34] B. Al-Ahmadi, A. Saleh and W. Al-Shammakh, Downhill Zagreb topological indices and M_{dn}-polynomial of some chemical structures applied for the treatment of COVID-19 patients, *Open J. Appl. Sci.* **10**(4) (2021) 108379.
[35] Ö. C. Havare, Quantitative structure analysis of some molecules in drugs used in the treatment of COVID-19 with topological indices, *Polycycl. Aromat. Compd.* **42** (2022) 5249–5260.
[36] K. G. Sreekumar and K. Manilal, Hosoya polynomial and Harary index of SM family of graphs, *J. Optim. Theory Appl.* **39**(2) (2018) 581–590.
[37] S.-J. Xu, H. Chen, Q.-X. Zhang and L. Tu, Hosoya polynomials of twisted toroidal polyhexes, *Ars Combin.* **114** (2014) 417–425.
[38] M. V. Diudea and I. Gutman, Wiener-type topological indices, *Croat. Chem. Acta* **71**(1) (1998) 21–51.
[39] M. Imran, M. Naeem, A. Q. Baig, M. K. Siddiqui, M. A. Zahid and W. Gao, Modified eccentric descriptors of crystal cubic carbon, *J. Discrete Math. Sci.* **22**(7) (2019) 1215–1228.